

Sortase D Forms the Covalent Bond That Links BcpB to the Tip of *Bacillus cereus* Pili*

Received for publication, February 9, 2009, and in revised form, March 5, 2009. Published, JBC Papers in Press, March 5, 2009, DOI 10.1074/jbc.M900927200

Jonathan M. Budzik¹, So-Young Oh, and Olaf Schneewind²

From the Department of Microbiology, University of Chicago, Chicago, Illinois 60637

Bacillus cereus and other Gram-positive bacteria elaborate pili via a sortase D-catalyzed transpeptidation mechanism from major and minor pilin precursor substrates. After cleavage of the LPXTG sorting signal of the major pilin, BcpA, sortase D forms an amide bond between the C-terminal threonine and the amino group of lysine within the YPKN motif of another BcpA subunit. Pilus assembly terminates upon sortase A cleavage of the BcpA sorting signal, resulting in a covalent bond between BcpA and the cell wall cross-bridge. Here, we show that the IPNTG sorting signal of BcpB, the minor pilin, is cleaved by sortase D but not by sortase A. The C-terminal threonine of BcpB is amide-linked to the YPKN motif of BcpA, thereby positioning BcpB at the tip of pili. Thus, unique attributes of the sorting signals of minor pilins provide Gram-positive bacteria with a universal mechanism ordering assembly of pili.

Sortases catalyze transpeptidation reactions to assemble proteins in the envelope of Gram-positive bacteria (1). Secreted proteins require a C-terminal sorting signal for sortase recognition such that sortase cleaves the substrate at a short peptide motif and forms a thioester-linked intermediate to its active site cysteine (2–4). Nucleophilic attack by an amino group within the bacterial envelope resolves the thioester intermediate, generating an amide bond tethering surface proteins at their C terminus onto Gram-positive bacteria (5). Four classes of sortases can be distinguished on the basis of sequence homology and substrate recognition (6, 7). Sortase A cleaves secreted protein at LPXTG sorting signals and recognizes the amino group of lipid II peptidoglycan precursors as a nucleophile (8, 9). Sortase B cleaves protein substrates at NPQTN sorting signals (10). This enzyme immobilizes proteins within fully assembled cell walls, utilizing the cell wall cross-bridge as a nucleophile (11). Sortase C cuts LPNTA sorting signals and anchors proteins to the peptidoglycan cross-bridges in sporulating bacteria (12, 13). Finally, sortase D catalyzes transpeptidation reactions in the assembly of pili (14, 15). Sortase D recognizes the amino group of lysine residues within the YPKN motif of pilin subunits as nucleophiles (16). The resultant sortase D-catalyzed amide bond links adjacent pilin subunits to grow the pilus fiber (16, 17).

Pili of Gram-positive bacteria comprised either two or three different pilin subunits synthesized as cytoplasmic precursors with N-terminal signal peptides and C-terminal sorting signals (P1 precursors) (14, 18). After translocation across the plasma membrane, P2 precursor species arise from removal of the signal peptide from P1 precursors by a signal peptidase (16). *Bacillus cereus* pili are composed of two subunits; that is, the major pilin, BcpA, and the minor pilin, BcpB (15). In contrast to BcpA, which is deposited throughout the pilus, BcpB is found at fiber tip (15). Sortase D cleaves the BcpA LPXTG motif sorting signal between the threonine and glycine residues to form an amide bond to the ϵ -amino group of the lysine within the YPKN motif of adjacent BcpA subunits (16). However, sortase A also cleaves BcpA precursors, which are subsequently linked to the side chain amino group of *meso*-diaminopimelic acid within lipid II (19). The latter reaction serves to terminate fiber elongation, immobilizing BcpA pili in the cell wall envelope (19).

The conservation of sortase D, the YPKN motif, and C-terminal sorting signal in major pilin subunits suggest a universal pilus assembly mechanism among Gram-positive bacteria (14, 20). However, the molecular mechanism whereby bacilli deposit BcpB, the minor pilin, at the tip of BcpA pili is not known. Although the BcpB precursor harbors an N-terminal signal peptide and a C-terminal IPNTG sorting signal, it lacks the YPKN pilin motif of the major subunit (15). Furthermore, the substrate properties of the BcpB IPNTG sorting signal for the four classes of sortases expressed by bacilli has yet to be established.

EXPERIMENTAL PROCEDURES

Plasmids—The following plasmids contain *B. cereus* pilus genes cloned under control of the *spac* promoter of pLM5 (12) and were described previously: pJB39 (*bcpA-srtD*), pJB12 (*bcpA-srtD-bcpB*), pJB28 (*bcpA_{K162A}-srtD-bcpB*), pJB32 (*bcpA-srtD_{C207A}-bcpB*), and pJB48 (*bcpA_{LAVAA}-srtD-bcpB*) (15). pJB182 encodes for *bcpA-srtD-bcpB_{ΔVIPNTGG719}*, which contains a seven-residue deletion in BcpB, encompassing the IPNTG sorting signal motif and one residue flanking each end (VIPNTGG⁷¹⁹). pJB12 was used as a template in site-directed mutagenesis with *Pfu* polymerase, as described previously (15), with primer pairs P128 and P129 Table 1. pJB139 encodes for *bcpA-srtD-bcpB* with a MH₆ tag inserted six nucleotides upstream from the codons encoding for the IPNTG motif in *bcpB*. pJB139 was created by quick change with primer pair P237/P238 and pJB12 template DNA. Amplified product was digested with *NheI* and ligated, and non-methylated plasmid DNA was digested with *DpnI* before transformation into *Escherichia coli* DH5- α . pJB139 was amplified with primer pairs

* This work was supported, in whole or in part, by National Institutes of Health Grant AI38897 (United States Public Health Service grant, to O. S.).

¹ A trainee of the National Institutes of Health Medical Scientist Training Program (Grant GM07281) at The University of Chicago.

² To whom correspondence should be addressed: Dept. of Microbiology, University of Chicago, 920 East 58th St., Chicago, IL 60637. Tel.: 773-834-9060; Fax: 773-834-8150; E-mail: oschnee@bsd.uchicago.edu.

TABLE 1

Primers used in this study

Lowercase letters indicate the sequence of the restriction site inserted. Italicized nucleotides encode for the MH₆ tag. Bold residues denote nucleotide changes introduced.

Primer	Restriction site	Nucleotide sequence (5'-3')
45	None	AAAAGTGGATGGATT ATTC CC AAAT ACGGGTGGTATAGGAACG
46	None	CGTTCCTATACCACCCG ATTC CG AAAT AATCCATCCACTTTT
47	PstI	AAActgcagAAGAATAATGGGTAAATTC
48	NheI	AAAgctagCCATGGTAATATACGATTTTC
88	KpnI	AAAggtaccAATACCTCCAAACAAGATTTTC
89	KpnI	AAAggtaccATCCTATTGTTATGTGTGTTCTA
105	None	AATAAAGTGGATGGAT TCTT GCGGTAGCGCT GGT ATAGGAACGACTCTT
106	None	AAGAGTCGTTCCCTATACC AGCCGC TAC CGCA AGAATCC ATCCACTTTTATT
124	None	GAGATTAACCGTGGTGC ATG GATTTAATAAAAACTGGTG
125	None	CACCAGTTTTTATAAAT CCAT GCACCACGTTAATCTC
128	None	AAAATGCAAGAATAATGGAGTGGACAACAATTTTTTAC
129	None	GTAAAAAATGTTGTTCCACTCCAATTTATCTTCGCACTTTT
173	None	TTATACAACTTAATTAC GCT ACGCCTTATGGAATAAAC
174	None	GTTTATTCATAAGGCGT AGCCG TAAATAAGTTGTATAA
197	None	TTCCACATGTATCCCA AGCT AGATTAACCGTGGTGCA
198	None	TGCACCAGTTTAACT CA GCTTTGGGATACATGTGAAC
237	NheI	AAAgctagcATGCATCCAT CA CCATCACTGGGTAATTC CTAATACTGGTG
238	NheI	AAAgctagcATTATCTTCGCACTTTTTCAGT
251	XbaI	AAAtctagaAAAATGCCTCCCTCTTTTCGATA
253	KpnI	AAAggtaccTTAGTCACGATGAATTCGGGG
254	PstI	AAActgcagCGGGAACATCTAATA
293	NcoI	AAAccatggTAATATACGATTTTCTTATAGAAATA

P105/106 to alter the sorting signal of BcpA, creating pJB202 (*bcpA_{LAVAA}-srtD-bcpB_{MH6}*). P197/198 and P124/125 were used with template pJB202 to introduce two substitutions in *bcpA* (N163A and V170M), creating pJB213 (*bcpA_{LAVAA N163A}-srtD-bcpB_{MH6}*). pJB174 encodes for *srtD-bcpB-gst* cloned in pLM5. pJB174 was created by amplification of *B. cereus* DNA with primers 251/293 and pGEX2T DNA with primers 294/253. Amplified DNA was digested with XbaI/NcoI and NcoI/KpnI, respectively and ligated into pLM5 digested with XbaI and KpnI. P254/253 were used to amplify *bcpB-gst* from the template pJB174. The amplified DNA was digested with PstI and KpnI and ligated into pJB12 also digested with PstI and KpnI, thereby generating pJB203 (*bcpA-srtD-bcpB-GST*). pJB205 (*bcpA-srtD_{C207A}-bcpB-GST*) contains the active site sortase D cysteine 207 to alanine substitution and was created by site-directed mutagenesis with pJB203 as a template and primers P173 and P174. pSY8 encodes for the cell wall sorting signal of BcpA fused to IsdX1 at its N terminus and GST³ at its C terminus. Plasmid pSY40 contains a substitution in the pentapeptide motif of the LPVTG motif of BcpA to the IPNTG motif of BcpB and was generated by quick change using pSY8 as a template and primers P45/P46. To swap the cell-wall sorting signal of BcpA with the cell-wall sorting signal of BcpB in pSY8, pSY8 (*isdX1-bcpA_{SS}-gst-srtD*) was digested with PstI and NheI. The BcpB cell-wall sorting signal was amplified with primers P47 and P48 and digested with PstI/NheI. The purified plasmid fragment was ligated with the digested BcpB PCR product resulting in pSY41. Plasmid variants lacking *srtD* were generated by QuikChangeTM. Primers P88/P89 with pSY40 or pSY41 as a template generated pSY51 (*isdX1-hybrid_{SS}-gst*) or pSY52

³ The abbreviations used are: GST, glutathione S-transferase; MALDI, matrix-assisted laser desorption ionization; HMW, high molecular weight; Ni-NTA, nickel-nitrilotriacetic acid; RP, reverse phase; HPLC, high performance liquid chromatography.

(*isdX1-bcpB_{SS}-gst*), respectively. Plasmids were transformed into the *dam⁻dcm⁻* *E. coli* host strain K1077 before transformation into *Bacillus anthracis* strain Sterne or its isogenic variant AHG263 (*srtA::ermC*).

Antisera—Polyclonal antisera to BcpA and BcpB were generated by injection of rabbits with purified His-tagged recombinant proteins (15).

Pilus Assembly—Bacilli were harvested after incubation for 20 h at 30 °C in the presence of 1.5 mM isopropyl 1-thio-β-D-galactopyranoside and 20 μM kanamycin. Bacilli were sedimented and boiled in 6 M urea, 1% SDS, 50 mM Tris-HCl, pH 9.5, for 10 min. The extracted material was washed with double-distilled H₂O, precipitated with 8% trichloroacetic acid, and washed once with 0.5 M Tris-HCl, pH 6.3, and then twice with 0.05 M Tris-HCl, pH 6.3. For immunoblots with α-BcpA and α-BcpB antisera, 3 ml of cell culture was digested with 100 units of mutanolysin in 0.05 M Tris-HCl, pH 6.3, 1.5 mM MgCl₂, and 1 mM phenylmethanesulfonyl chloride. For purification of BcpB_{MH6}-BcpA from *B. anthracis* strains harboring pJB213, 6 liters of cell culture were digested with 20,000 units of mutanolysin, and cells were processed as described previously (19). Reactions were incubated at 37 °C for 16 h, and the solubilized cell wall species was subjected to immunoblotting and purified by Ni-NTA affinity chromatography. For immunoblots of pili from *B. anthracis* Sterne variants (*srtA::ermC*), aliquots were precipitated with 7% trichloroacetic acid, incubated on ice for 30 min, and centrifuged at 16,000 × g for 10 min. The sediment was washed with 500 μl of acetone, air-dried, and suspended in 500 μl of 4% SDS, 50 mM Tris-HCl, pH 8.0.

Purification of BcpB_{MH6}-BcpA—After cell wall digestion, insoluble material was removed by centrifugation at 33,000 × g. The pH of the sample was adjusted to 7.5 with 2 M sodium phosphate dibasic, and BcpB_{MH6}-BcpA was purified by Ni-NTA affinity chromatography (11).

Purification of BcpB-BcpA Peptides—Purified BcpB_{MH6}-BcpA was methanol-chloroform-precipitated and cleaved with CNBr (11). BcpB_{H6}-BcpA was purified by a second round of Ni-NTA affinity chromatography under denaturing conditions and separated by reverse-phase high performance liquid chromatography (RP-HPLC) with UV detection using a C18 column with a linear gradient from 1 to 99% acetonitrile (CH₃CN) in 0.1% formic acid in 100 min, as previously reported for BcpA pilin peptides (16) and the BcpA anchor structure (19).

Mass Spectrometry—Aliquots of RP-HPLC fractions (0.5 μl) were co-spotted with matrix (0.5 μl of α-cyano-4-hydroxycinnamic acid) prepared at 10 mg/ml in CH₃CN-water-trifluoroacetic acid (30:40:0.1). Matrix-assisted laser desorption ionization (MALDI)-mass spectrometry spectra were obtained in a reflectron time-of-flight instrument (ABI Biosystems MALDI 4700) in reflectron mode. Spectra were acquired using external calibration with bovine insulin. Theoretical parent ion and fragmentation ion monoisotopic *m/z* values were produced with ProteinProspector version 5.1.8 Basic MSProduct web-based program (University of California, San Francisco).

Edman Degradation—RP-HPLC samples of anchor peptides were dried under vacuum and submitted for Edman sequencing at the University of Illinois, Urbana-Champaign Biotechnology Center Protein Sciences Facility. IsdX1-BcpB_{SS}-GST cleavage

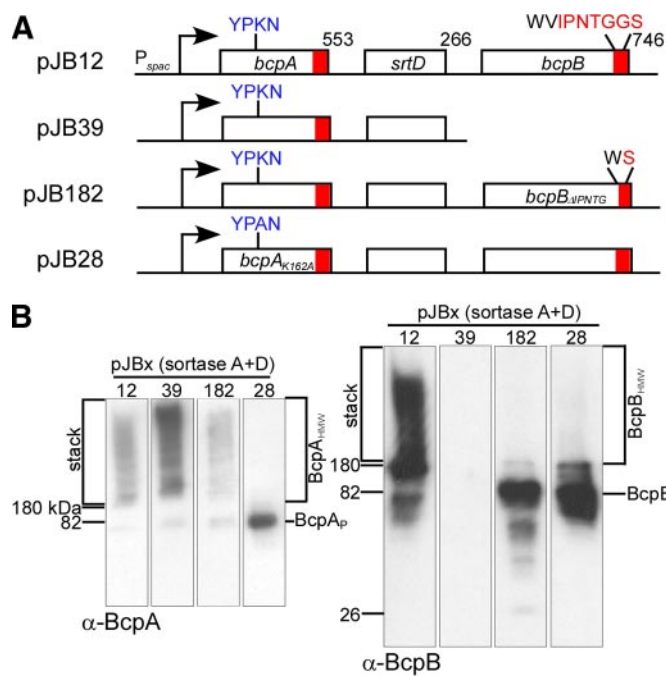


FIGURE 1. The IPNTG motif sorting signal of BcpB is required for the incorporation of BcpB into pili. *A*, schematic of plasmids expressing pilin genes under control of the isopropyl 1-thio- β -D-galactopyranoside-inducible P_{spac} promoter. pJB12 expressed wild-type *bcpA-srtD-bcpB*, and pJB39 expressed *bcpA-srtD*. pJB28 contains a substitution in the pilin motif lysine (*bcpA*_{K162A}-*srtD-bcpB*). The cell wall sorting signal pentapeptide motif in BcpB was deleted in plasmid pJB182 (*bcpA-srtD-bcpB* _{Δ IPNTG}). Cell wall sorting signals in BcpA and BcpB are colored red. The YPK pilin motif in BcpA is colored blue. *B*, *B. anthracis* cell wall extracts were digested with mutanolysin. BcpA and BcpB pilus material was separated by SDS-PAGE and analyzed by immunoblot with α -BcpA and α -BcpB antisera. BcpA and BcpB high molecular weight material (HMW) and precursor species (P) are indicated. The electrophoretic mobility of the marker is indicated.

products were transferred to a polyvinylidene difluoride membrane, stained with Amido Black, and submitted for Edman degradation.

Electron Microscopy—Double labeling experiments with α -BcpA antisera and 10-nm gold anti-rabbit IgG conjugates followed by α -BcpB antisera and 15-nm gold anti-rabbit IgG conjugates were performed as described previously (15).

RESULTS

The Sorting Signal of the Minor Pilin Is Required for Its Assembly into Pili—When transformed with pJB12, a plasmid encoding the *B. cereus* pilin operon (*bcpA*, *srtD*, *bcpB*), *B. anthracis* Sterne forms pili comprising both the major pilin subunit, BcpA, and the minor pilin subunit, BcpB (Fig. 1A) (15). Lysates of bacilli were examined by SDS-PAGE and immunoblotting for the polymerization of pilin subunits. High molecular weight BcpA_{HMW} and BcpB_{HMW} species represent covalently linked pilin subunits within pilus fibers (Fig. 1B). As expected, *B. anthracis* expressing *bcpA* and *srtD* but not *bcpB* (pJB39) formed exclusively BcpA_{HMW} species, indicating that the major pilin is polymerized in the absence of BcpB (Fig. 1B) (15). Substitution of lysine 162 of BcpA (K of the YPKN pilin motif) with alanine (pJB28, *bcpA*_{K162A}, *srtD*, *bcpB*) abrogates polymerization of both BcpA_{K162A} and BcpB into high molecular weight species (BcpB_{HMW}) and caused the accumulation of pilin precursors, BcpA_P and BcpB_P (Fig. 1B) (15). Deletion of

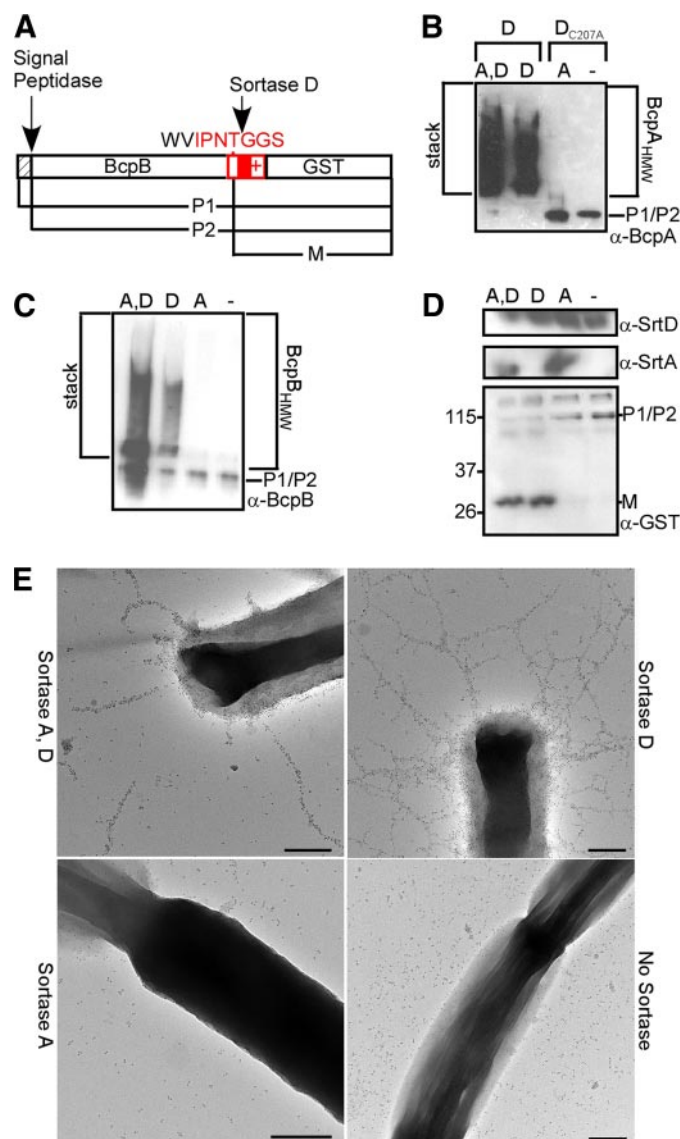


FIGURE 2. Cleavage of BcpB-GST by sortase D and the contribution of sortases to pilus assembly. *A*, the diagram displays the precursor (P1) of BcpB-GST and the signal peptidase (P2) and sortase-cleaved products (M). *B* and *C*, pilus formation from BcpA and BcpB substrates was examined by immunoblotting with α -BcpA (*B*) or α -BcpB (*C*) sera in cells harboring both sortase D (SrtD) and sortase A (SrtA), only one of the two active sortases (SrtD_{C207A} contains a mutation in the active site cysteine), or none at all. *D*, cytoplasmic and membrane fractions were examined by immunoblotting with α -SrtD, α -SrtA, or α -GST sera. Electrophoretic mobility of the molecular weight marker, pilin precursors (P1/P2), and mature cleavage products (M) on SDS/PAGE is indicated. *E*, bacilli were examined by immunogold labeling with α -BcpA serum and viewed by transmission electron microscopy. Scale bars, 500 nm.

the IPNTG peptide in the sorting signal of BcpB (pJB182, *bcpA*, *srtD*, *bcpB* _{Δ IPNTG}) abolishes the formation of BcpB_{HMW} without affecting BcpA polymerization (Fig. 1B). Thus, the BcpB C-terminal sorting signal is required for the incorporation of the minor pilin subunit into pili but is otherwise dispensable for the polymerization of BcpA.

The BcpB Sorting Signal Is Cleaved by Sortase D—To examine BcpB sorting signal cleavage, we generated a translational hybrid between the minor pilin 3' coding end and the 5' end of glutathione *S*-transferase (*gst*) (Fig. 2A). *B. anthracis* Sterne (wild-type sortase A) and an isogenic *srtA* deletion variant

BcpB Linkage to Pilus Tip

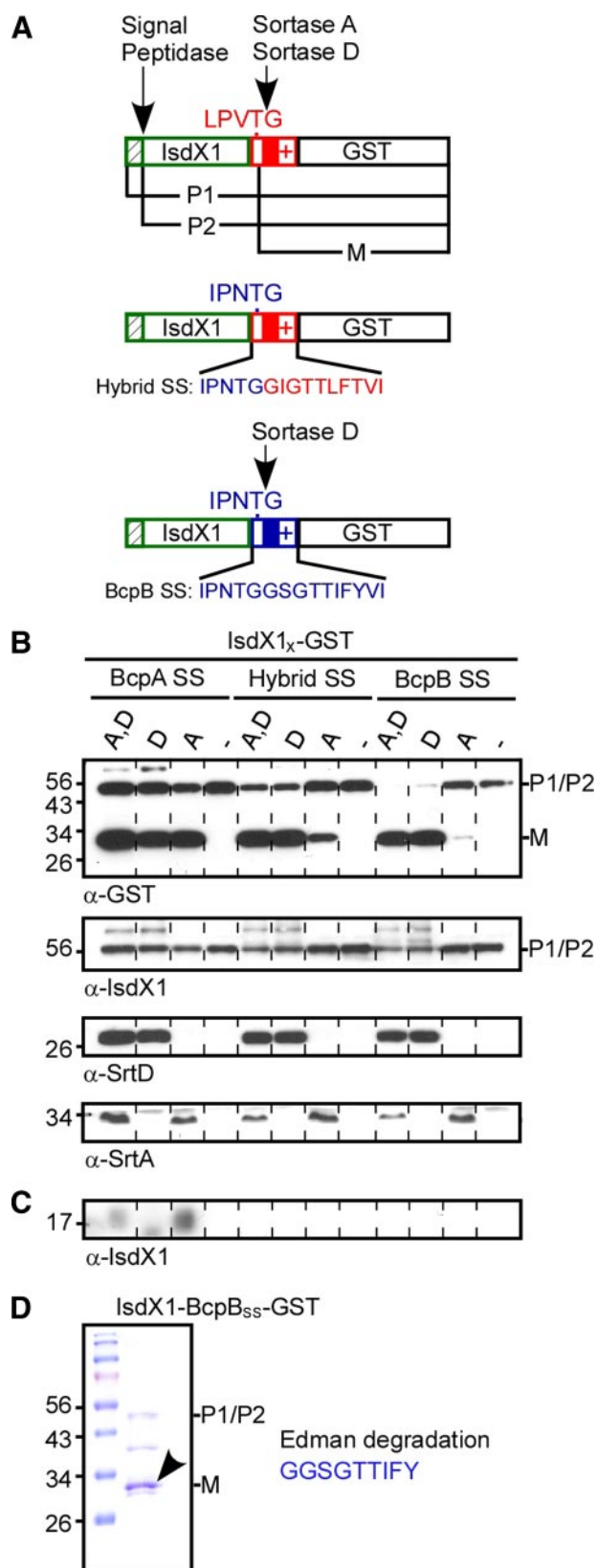


FIGURE 3. IsdX1-BcpB_{SS}-GST is cleaved by sortase D. *A*, IsdX1-BcpA_{SS}-GST is a translational hybrid between IsdX1 (green), the cell-wall sorting signal of BcpA (red; IsdX1-BcpA_{SS}-GST), or the cell wall sorting signal of BcpB (blue; IsdX1-BcpB_{SS}-GST) and glutathione *S*-transferase. IsdX1-Hybrid_{SS}-GST is a hybrid between IsdX1, the cell-wall sorting signal of BcpA with alteration of the LPVVTG motif to IPNTG, and glutathione *S*-transferase. The diagram displays the precursor (P1) of IsdX1_{SS}-GST and the signal peptidase (P2) and

(*srtA::ermC*) (21) were transformed with plasmids encoding the BcpB-GST hybrid, BcpA, and either wild-type sortase D (*bcpA*, *srtD*, *bcpB-gst*) or the active site mutant, C207A (*bcpA*, *srtD*_{C207A}, *bcpB-gst*). Pilus assembly in bacilli was assessed by immunoblotting as before. Wild-type sortase D assembled BcpA_{HMW}, whereas the C207A variant of sortase D did not form pili and accumulated the BcpA precursor (Fig. 2*B*). Similarly, wild-type sortase D yielded BcpB_{HMW}, whereas the C207A sortase D variant accumulated BcpB-GST precursor (Fig. 2*C*). Immunoblotting with antibodies raised against purified GST detected the BcpB-GST precursor (P1/P2) as well as the mature C-terminal GST fragment released by sortase D cleavage (*M*, Fig. 2*D*). In contrast, bacilli expressing the C207A sortase D variant were unable to process minor subunit precursors. Furthermore, BcpB-GST cleavage is independent of sortase A, indicating that sortase D, but not sortases A, B, or C, is able to recognize BcpB substrate (Fig. 2*D*). Electron microscopy of immunogold labeled pili on the surface of bacilli demonstrates that GST fusion to the C terminus of BcpB does not affect pilus assembly (Fig. 2*E*). Mutants lacking sortase A successfully assemble pili on the bacterial surface, although they are abundantly shed into the extracellular medium (Fig. 2*E*). Mutants expressing the C207A variant of sortase D fail to form pili (Fig. 2*E*).

The BcpB Sorting Signal Determines Sortase D Substrate Specificity—*B. anthracis* as well as closely related *B. cereus* species secrete IsdX1, a hemophore that scavenges heme iron from host hemoglobin (22). We selected IsdX1 as a reporter because this protein is known to travel along the bacterial secretory pathway but is not associated with pili. IsdX1-BcpA_{SS}-GST is a translational hybrid between IsdX1, the sorting signal of BcpA (BcpA_{SS}) and *E. coli* glutathione *S*-transferase (Fig. 3*A*) (19). Cleavage of the hybrid precursor (P1/P2) into the mature form (*M*) was monitored by immunoblotting with α-GST serum (Fig. 3*A*). IsdX1-BcpA_{SS}-GST was cleaved in bacilli expressing sortase A and/or sortase D, indicating that the sorting signal of BcpA is recognized by both sortases (Fig. 3*B*) (19). The LPVVTG peptide within BcpA_{SS} was replaced with IPNTG, the peptide found in the BcpB sorting signal, thereby creating IsdX1-Hybrid_{SS}-GST (Fig. 3*A*). Sortase A cleaves the IsdX1-Hybrid_{SS}-GST less efficiently than the IsdX1-BcpA_{SS}-GST. However, the abundance of mature products in bacilli expressing sortase D appeared similar for both substrates (Fig. 3*B*). A third fusion, IsdX1-BcpB_{SS}-GST, encompasses the sorting signal of BcpB. This hybrid was cleaved in bacilli expressing sortase D but not in bacteria that lacked this transpeptidase (Fig. 3*B*). In bacilli expressing IsdX1-BcpA_{SS}-GST, sortase A attached IsdX1 to the cell wall envelope. In contrast, sortase A-mediated cell wall

sortase-cleaved products (*M*). *B. sortase* cleavage products were detected in urea-SDS-released cytoplasmic and membrane fractions by immunoblotting with α-GST antiserum. Antisera raised against *B. cereus* sortase D and *B. anthracis* sortase A allowed for their detection by immunoblotting. Labels indicate the sortase (*srtA*, *srtD*, or none) and substrate (*isdX1_{SS}-gst* with BcpA, BcpB, or hybrid cell wall-sorting signals) expressed in each strain. *C*, *Bacillus* cell wall extracts were digested with mutanolysin. IsdX1 anchoring was analyzed by immunoblot with α-IsdX1 antibodies. *D*, affinity chromatography of IsdX1-BcpB_{SS}-GST from bacilli on glutathione-Sepharose revealed P1/P2 and mature (*M*) species, the latter of which was analyzed by Edman degradation. The experimentally determined amino acid sequences is printed in blue.

anchoring of IsdX1 could not be detected in bacilli expressing either IsdX1-Hybrid_{SS}-GST or IsdX1-BcpB_{SS}-GST (Fig. 3C). Lysates of *B. anthracis* Sterne expressing IsdX1-BcpB_{SS}-GST were subjected to affinity chromatography on glutathione-Sepharose. Eluate was analyzed by Coomassie-stained SDS-PAGE, which revealed the P1/P2 precursors (50 kDa) and the mature sortase D-derived C-terminal cleavage fragment of IsdX1-BcpB_{SS}-GST (31 kDa, Fig. 3D). The 38-kDa polypeptide in the eluate likely represents *B. anthracis* GST; this species did not react with antibodies against IsdX1 or *E. coli* GST (Fig. 3B). Edman degradation of the 31-kDa C-terminal sortase D cleavage product of IsdX1-BcpB_{SS}-GST generated the amino acid sequence GSGTTFIFY, which matches the predicted sequence of the BcpB_{SS} immediately after the threonine of the IPNTG motif (Table 2). Thus, sortase D cleaves the BcpB sorting signal between the threonine and the glycine of its IPNTG sorting signal.

Sortase D Incorporates BcpB into Pili of *B. anthracis*—We asked whether BcpB is incorporated into pili in the absence of sortase A, *i.e.* when these fibers cannot be immobilized in the

TABLE 2
Edman degradation of IsdX1-BcpB_{SS}-GST product of sortase D

Cycle	Amino acid
1	Gly (15.28)
2	Gly (14.81)
3	Ser (7.39)
4	Gly (12.14)
5	Thr (17.77)
6	Thr (17.21)
7	Ile (14.10)
8	Phe (11.06)
9	Tyr (10.45)

cell wall envelope. *B. anthracis* (*srtA::ermC*) was transformed with pJB12 (*bcpA*, *srtD*, *bcpB*) or pJB39 (*bcpA*, *srtD*) (Fig. 4A). The *srtA* mutant bacilli released pili derived from either plasmid into the culture medium (Fig. 4C). Pili in the medium were precipitated with trichloroacetic acid and examined by immunoblot probed with α -BcpB and α -BcpA antisera (Fig. 4B). BcpA_{HMW} was identified within polymerized pili derived from both plasmids, whereas BcpB_{HMW} was only detected in the pili of pJB12 (*bcpA*, *srtD*, *bcpB*) transformants (Fig. 4B). The localization of BcpB in both cell-associated pili and released pili was established via immunogold labeling and electron microscopy. BcpA was detected with 10-nm immunogold conjugates along the shaft of pili that were displayed on the surface of bacilli or released into the culture medium (Fig. 4C). BcpB was detected with 15-nm immunogold conjugates at the tip of pili that were either displayed on the bacterial surface or released into the culture medium (Fig. 4C). BcpB-specific immunogold labeling was not detected in pili that were formed without *bcpB* (pJB39) (Fig. 4C). Together, these results suggest that sortase A is dispensable for the incorporation of BcpB into pili and that BcpB is deposited at the tip of BcpA pili irrespective of pilus surface attachment.

The Bond between BcpB and BcpA—*B. anthracis* (pJB48) encodes a mutant BcpA with a scrambled LPXTG motif sorting signal (LAVAA) that cannot be cleaved by sortases A and D and, consequently, cannot be incorporated into pili or the cell wall envelope (Fig. 5A) (15). As expected, immunoblotting of *B. anthracis* (pJB48) cell wall extracts did not reveal polymerized BcpA_{HMW} or BcpB_{HMW} (Fig. 5B) (15). Nevertheless, *B. anthracis* (pJB48) accumulated a 180-kDa species immunoreactive against both BcpA and BcpB sera (15). We reasoned these species must represent the sortase D transpeptidation product BcpB-BcpA_{LAVAA} (15). If so, purification and biochemical analysis of this transpeptidation product may reveal the chemical bond that tethers BcpB to BcpA pili.

To pursue this goal, we inserted an MH₆ tag two residues upstream of the IPNTG sorting signal of BcpB within plasmid pJB202 (*bcpA*_{LAVAA}, *srtD*, *bcpB*_{MH6}) (Fig. 5A). Asparagine 163 (Y_{PKN}¹⁶³) of BcpA forms an intramolecular isopeptide bond that is dispensable for pilus assembly, as substitution of asparagine 163 with alanine abolished isopeptide bond formation without affecting pilus assembly (16). As expected, introduction of the *bcpA* N163A mutation in pJB213 (*bcpA*_{N163A}, *LAVAA*, *srtD*, *bcpB*_{MH6}) had no effect on the ability of sortase D to generate the transpeptidation product BcpB_{MH6}-BcpA_{LAVAA} (Fig. 5, A and B). As a control, the His-horseradish peroxidase probe identified both BcpB_{MH6} precursor and

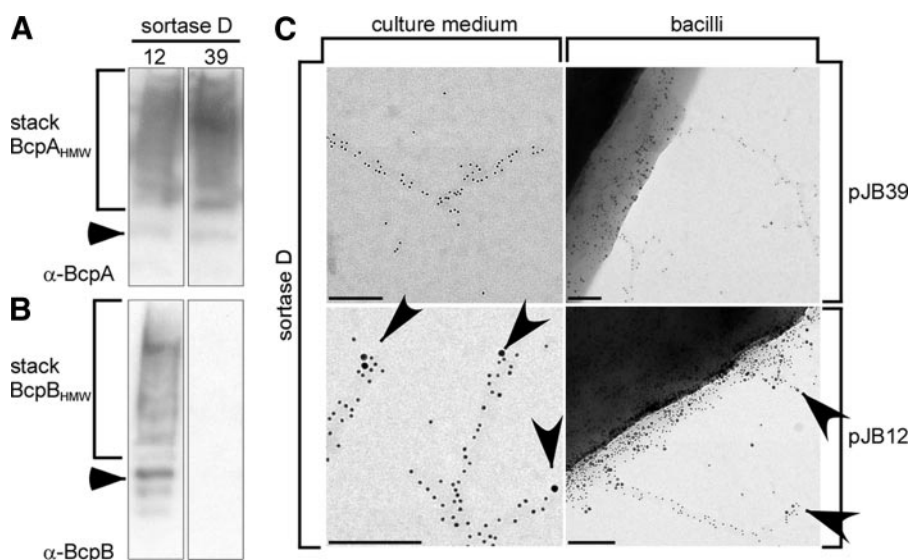


FIGURE 4. SrtA is not required for the incorporation of BcpB into pilus fibers. A, plasmids expressing pilin genes under control of the P_{spac} promoter were analyzed by immunoblot for pilus assembly in sortase A-mutant bacilli. pJB39 (39) expresses *bcpA-srtD*, whereas pJB12 (12) also expresses *bcpB* (see Fig. 1 for the schematic). Pili released into the medium were precipitated, separated by SDS-PAGE, and immunoblotted with α -BcpA (A) and α -BcpB (B). BcpA and BcpB high molecular weight material (HMW) and precursor species (arrowheads) are indicated. The electrophoretic mobility of the marker is indicated. C, pili released into the medium or attached to cells were labeled with α -BcpA serum and 10-nm gold anti-rabbit conjugate followed by α -BcpB serum and 15-nm gold conjugate. Arrowheads indicate 15-nm gold particles detected in pili from *B. anthracis* (*srtA::ermC*) (pJB12). Scale bars, 200 nm.

BcpB Linkage to Pilus Tip

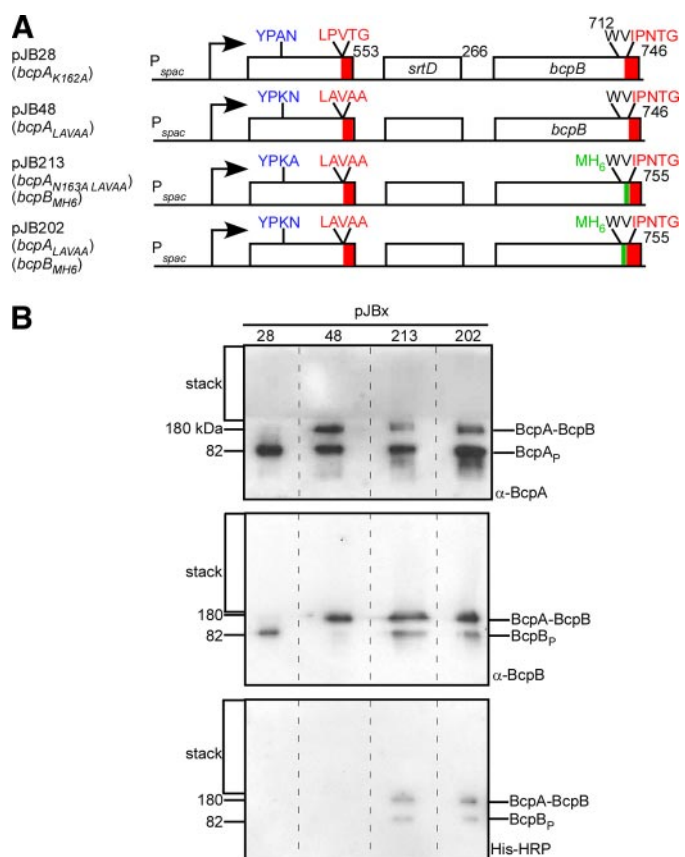


FIGURE 5. Formation of BcpB-BcpA_{LAVAA} intermediates in *B. anthracis*. A, schematic of plasmids expressing pilin genes under control of the P_{spac} promoter. pJB28 expresses *bcpA* with the YPKN motif altered to YPAN (*bcpA*_{K162A}-*srtD*-*bcpB*). pJB48 contains *bcpA* with an intact YPKN motif but harbors a scrambled sorting signal (*bcpA*_{LAVAA}-*srtD*-*bcpB*). A MH₆ peptide was inserted two residues upstream from the IPNTG motif sorting signal of *bcpB* in pJB202, which also contained the scrambled sorting signal in *bcpA* (*bcpA*_{LAVAA}-*srtD*-*bcpB*_{MH6}). The YPKN motif in *bcpA* encoded by pJB202 was altered to YPKA, creating pJB213 (*bcpA*_{N163A LAVAA}-*srtD*-*bcpB*_{MH6}). B, cell wall extracts were digested with mutanolysin. Samples were separated by SDS-PAGE and immunoblotted with α-BcpA sera, α-BcpB sera, and His-horseradish peroxidase (HRP) probe. BcpB-BcpA_{LAVAA} (BcpA-BcpB) and precursor species (P) are indicated. The electrophoretic mobility of the marker is indicated.

BcpB_{MH6}-BcpA_{LAVAA} in cell wall extracts from bacilli harboring pJB202 or pJB213 (Fig. 5B).

Bacillus extracts containing BcpB_{MH6}-BcpA_{N163A, LAVAA} were subjected to affinity chromatography on Ni-NTA-Sepharose (Fig. 6A). The eluate was analyzed by Coomassie-stained SDS-PAGE, which demonstrated purification of the BcpB_{MH6}-BcpA_{N163A, LAVAA} transpeptidation product (Fig. 6A). Eluted transpeptidation product was cut at methionyl residues with cyanogen bromide (CNBr), and cleavage products were subjected to a second round of Ni-NTA affinity chromatography (Fig. 6A). Eluted peptides were further purified by RP-HPLC with UV detection at 215 nm (Fig. 6A). At 20% acetonitrile, 0.1% formic acid, a peak of 15–20 milliabsorbance units was detected, and the compound was subjected to MALDI-mass spectrometry (Fig. 6, A and B). The predominant ion signal at 2764.68 *m/z* was identified as the branched peptide HHHHHH-HWVIPNT(YPKAEIKRGAM*) containing the tryptophan oxidation product hydroxytryptophan (calculated monoisotopic *m/z* 2764.41) (Fig. 6C). An additional cluster of peaks at 2782.69 *m/z* is thought to represent the branched peptide containing

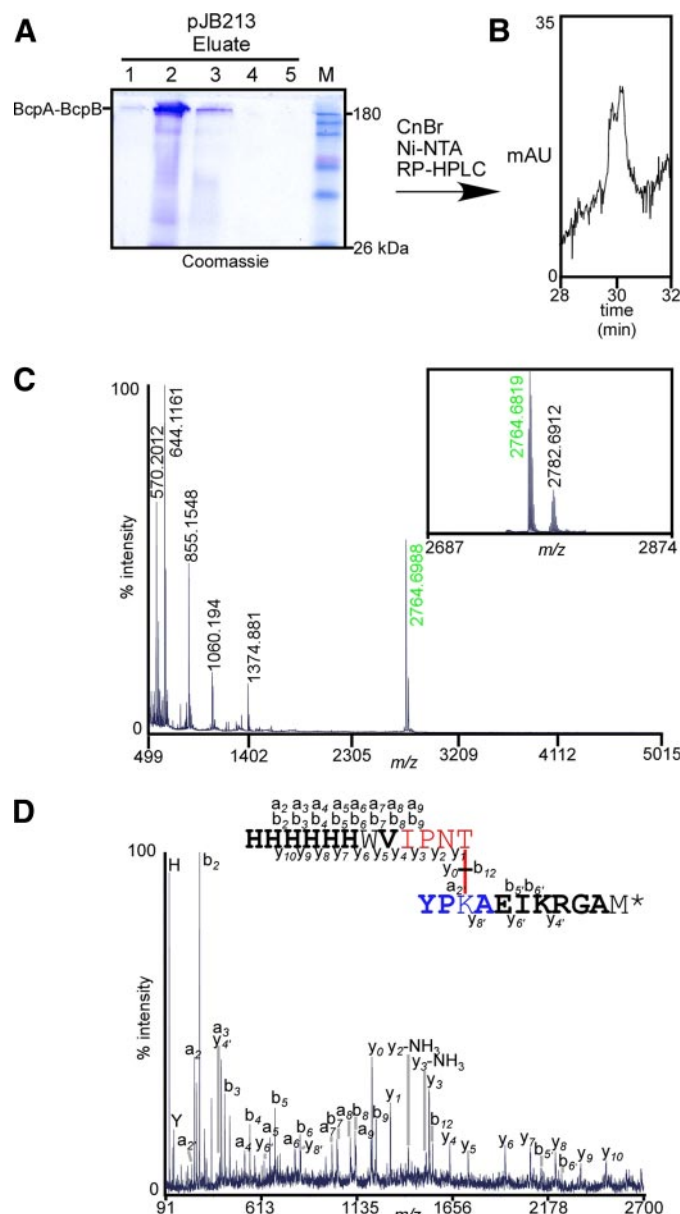


FIGURE 6. An amide bond assembles BcpB and BcpA. A, BcpB_{MH6}-BcpA_{LAVAA} was purified by Ni-NTA affinity chromatography from cell wall extracts treated with mutanolysin. Purified product was analyzed by SDS-PAGE and stained with Coomassie. The linked pilin proteins (BcpA-BcpB) and electrophoretic mobility of the marker are indicated. B, purified proteins were cleaved with CNBr, purified by a second round of Ni-NTA, and subjected to RP-HPLC with UV detection at 215 nm. mAU, milliabsorbance units. C, peptides that eluted at 20% acetonitrile, 0.1% formic acid were analyzed by MALDI-mass spectrometry. D, collisionally activated dissociation fragmentation spectrum of parent ion 2764.68 *m/z*.

homoseril instead of homoseril lactone, methionyl reaction products that are acquired during CNBr cleavage (Fig. 6C) (16). The ion signal at 2764.68 *m/z* was fragmented via collisionally activated dissociation, and fragment ion spectra confirmed the predicted structure of the branched peptide displayed in Fig. 6D and Table 3). The *b*₅- and *b*₆- fragment ions revealed that the YPKN motif lysine residue 162 of BcpA participates in an amide bond with the C-terminal threonine (residue 717) of BcpB (Lys¹⁶²-Thr⁷¹⁷) (Table 3; Fig. 6D). The branched peptide was further analyzed by Edman degradation, which released

TABLE 3

Summary of ions produced during MS/MS of the mutanolysin-released m/z 2764.68 parent ion

m/z		$A_{\text{obs}} - \text{calc}^a$	Ion type ^b	Proposed structure ^c
Observed	Calculated			
70.14	70.07	0.07	Immonium	Pro or Arg
84.15	84.08	0.07	Immonium	Lys
86.18	86.10	0.09	Immonium	Ile
110.16	110.07	0.09	Immonium	His
129.20	129.10	0.10	Immonium	Lys
136.16	136.08	0.08	Immonium	Tyr
230.29	230.11	0.18		GAM*
233.19	233.13	0.06	y_3'	YP
247.24	247.13	0.11	a_2	HH
275.23	275.13	0.11	b_2	HH
302.28	302.15	0.13	i	WV
312.24	312.16	0.09	i	KAE-NH ₃
313.29	313.15	0.14	i	PNT
340.25	340.14	0.11	i	HW
384.26	384.19	0.07	a_3	HHH
386.25	386.21	0.03	y_4'	RGAM*
412.32	412.18	0.13	b_3	HHH
439.34	439.21	0.13	i	HWV
477.32	477.20	0.12	i	HHW
514.26	514.31	-0.05	y_5'	KRGAM*
521.42	521.25	0.17	a_4	HHHH
549.38	549.24	0.14	b_4	HHHH
576.39	576.27	0.13	i	HHWV
627.47	627.39	0.07	y_6'	IKRGAM*
658.46	658.31	0.15	a_5	HHHHH
686.43	686.30	0.13	b_5	HHHHH
713.45	713.33	0.12	i	HHHWV
756.45	756.44	0.02	y_7'	EIKRGAM*
795.45	795.37	0.09	a_6	HHHHHH
823.55	823.36	0.19	b_6	HHHHHH
827.58	827.47	0.10	y_8'	AEIKRGAM*
963.55	963.47	0.08	i	HHHHWVI
997.63	997.44	0.19	a_7	HHHHHHW
1025.62	1025.44	0.18	b_7	HHHHHHW
1097.71	1096.51	1.20	b_8	HHHHHHWV
1124.70	1124.50	0.19	b_8	HHHHHHWV
1209.88	1209.59	0.28	a_9	HHHHHHWVI
1215.89	1215.68	0.21	y_0	YPKAEIKRGAM*
1237.83	1237.59	0.24	b_9	HHHHHHWVI
1316.92	1316.73	0.19	y_1	T(YPKAEIKRGAM*)
1413.98	1413.75	0.23	y_2 -NH ₃	NT(YPKAEIKRGAM*)
1511.16	1510.80	0.35	y_3 -NH ₃	PNT(YPKAEIKRGAM*)
1528.14	1527.83	0.32	y_3	PNT(YPKAEIKRGAM*)
1531.25	1531.72	-0.47	b_{12} -H ₂ O	HHHHHHWVIPNT
1641.18	1640.91	0.27	y_4	IPNT(YPKAEIKRGAM*)
1741.21	1739.98	1.23	y_5	VIPNT(YPKAEIKRGAM*)
1942.49	1942.05	0.44	y_6	WVIPNT(YPKAEIKRGAM*)
2079.61	2079.11	0.50	y_7	HWVIPNT(YPKAEIKRGAM*)
2138.62	2138.02	0.60	b_5'	HHHHHHWVIPNT(YPKAEI)
2216.77	2216.17	0.59	y_8	HHWVIPNT(YPKAEIKRGAM*)
2235.67	2235.16	0.52	i	HHHWVIPNT(YPKAEIKRGA)-NH ₃
2251.66	2251.11	0.56	b_6'	HHHHHHWVIPNT(YPKAEI)
2354.38	2353.23	1.15	y_9	HHHWVIPNT(YPKAEIKRGAM*)
2491.31	2490.29	1.01	y_{10}	HHHHWVIPNT(YPKAEIKRGAM*)

^a The difference between observed and calculated monoisotopic m/z values.^b i denotes internal ions.^c Trp is modified as hydroxytryptophan. M* represents a homoserine lactone residue.

two amino acids per cleavage during the first two reaction cycles (Fig. 6D; Table 4). In the third cycle, histidine was identified; however lysine (Lys¹⁶²) was not released during Edman degradation, as this residue is engaged in an amide bond with BcpB T⁷¹⁷ (Fig. 6C; Table 4). In cycle 7 Edman degradation released the lysine of Lys¹⁶⁶, which is not amide-bonded to BcpA (Fig. 6D, Table 4). Tryptophan was not identified in cycle 7 because this residue is degraded during the Edman cycle (Table 4) (19). In summary, these results demonstrate that BcpB and BcpA are linked via an amide bond between the C-terminal threonine of BcpB and the ϵ -amino group of lysine within the YPKN motif of BcpA (Lys¹⁶²-Thr⁷¹⁷) (Fig. 6D).

TABLE 4
Edman degradation of BcpB-BcpA branched peptide

Cycle	Amino acid
	<i>PM</i>
1	His (10.32), Tyr (13.93)
2	His (9.68), Pro (8.56)
3	His (7.39)
4	His (6.77), Ala (8.59)
5	His (7.14), Glu (6.77)
6	His (6.44), Ile (5.79)
7	Lys (3.51)
8	Val (2.41), Arg (24.00)
9	Gly (2.29)
10	Ala (2.53)

DISCUSSION

Many Gram-positive bacteria elaborate pili and thereby adhere to and invade host tissues or form biofilms (23). Minor pilin subunits are critically important for bacterial adherence to host cell surfaces, which is also a prerequisite for invasion or biofilm formation (24–27). For example, the minor pilin subunit of *Streptococcus agalactiae* provides for bacterial adherence to the brain endothelium as well as pulmonary epithelial cells (28, 29). *Corynebacterium diphtheriae* assemble pili from three subunits, the major pilin SpaA, and two minor pilins, SpaC and SpaB (14). SpaC is deposited at the tip of SpaA pili, whereas SpaB is found in regular intervals along the pilus shaft (14). Both SpaC and SpaB are required for corynebacterial adherence to pharyngeal cells, a process that does not depend on the SpaA subunit (30). Another minor pilin subunit, RrgA of *Streptococcus pneumoniae*, promotes bacterial adherence to respiratory epithelia (31). RrgA has been reported to bind to the extracellular matrix components fibronectin, collagen I, and laminin (32). Finally, Group A streptococcal pili engage the scavenger receptor gp340 on pharyngeal cells to promote adherence and aggregation (33). Although minor pilins appear generally involved in pilus-mediated adherence, there are exceptions to this, as the major pilin subunit of *S. pneumoniae* pilus islet-2 (PI-2) mediates bacterial adherence to lung epithelial cells (34).

We have focused on *B. cereus* and its close relative *B. anthracis* to study the assembly of pili in Gram-positive bacteria. Bacilli form pili from two subunits, the major pilin BcpA and the minor pilin BcpB. We show here that the sorting signal of the minor pilin is recognized by sortase D, which subsequently cleaves its substrate between the threonine and the glycine residues of its IPNTG motif. The product of this reaction, a thioester-linked acyl enzyme, is resolved by the nucleophilic attack of the ϵ -amino group of lysine with the YPKN pilin motif of BcpA. The aforementioned reaction is not absolutely dependent on the LPVTG sorting signal of BcpA (15). We took advantage of this observation and purified the sortase D-catalyzed transpeptidation product BcpB_{MH6}-BcpA_{LAVAA} using a BcpA sorting signal variant that cannot be used as substrate for further polymerization. Mass spectrometry and Edman degradation of affinity-purified BcpB_{MH6}-BcpA_{LAVAA} revealed the amide bond that tethers the minor pilin subunit to the tip of BcpA pili.

The observation that the IPNTG sorting signal of BcpB is recognized by sortase D, but not by sortase A, provides a compelling argument for a model that may be universally applicable for pilus assembly in Gram-positive bacteria. Biochemical analysis of sortase-catalyzed transpeptidation reactions revealed that resolution of acyl intermediates is the rate-limiting activity of sortase (35). Thus, if BcpB were the preferred substrate of sortase D, its intermediates could only be resolved by the nucleophilic attack of the amino group of BcpA, generating BcpB-BcpA transpeptidation products and positioning BcpB at the tip of pili. Sortase D can only accept one nucleophile, the ϵ -amino group of lysine within the YPKN pilin motif of BcpA. As a consequence, sortase D cleavage of BcpB-BcpA must be followed by further polymerization with major pilin subunits,

resulting in the formation of BcpB-BcpA_{n+1}. In contrast to BcpB, the BcpA LPVTG sorting signal can be cleaved by both sortase D and sortase A, the latter of which recognizes the side chain amino group of *m*-diaminopimelic acid within lipid II as a nucleophile to resolve its acyl intermediates (19). This reaction was recently demonstrated by studying the sortase A-catalyzed cell wall anchor structure of the major pilin subunit BcpA (19). Thus, competition between two transpeptidases, sortase D and sortase A, for the same pilin subunit can be viewed as a determinant for both pilus length and cell wall anchoring of fully assembled fibers. We propose that this model may be universally applicable to the assembly of pili in all Gram-positive bacteria. Pili in *B. cereus*, *Actinomyces spp.*, and some group A streptococcal isolates are formed from two pilin subunits (36, 37). However, other Gram-positive bacteria assemble pili from three subunits (38). *C. diphtheriae* pili are formed via polymerization of the major subunit, SpaA. One of the minor subunits, SpaC, is deposited at the tip, whereas another minor pilin, SpaB, is incorporated at regular intervals along the shaft of polymerized SpaA (14). Recent work suggests that SpaB encompasses a side chain amino group that functions as a nucleophile, producing reiterative covalent links between SpaA and SpaB subunits (39). Nevertheless, it is still not clear whether pilin-specific sortases recognize the side chain amino groups of both major and minor pilins as nucleophiles to resolve their intermediates. Furthermore, the amide bonds that are formed during the assembly of pili comprising three subunits must be revealed.

Acknowledgments—We thank Valerie Anderson, Bill Blaylock, and Gabriella Garufi for critical comments on this manuscript. We acknowledge membership within and support from the Region V Great Lakes Regional Center of Excellence in Biodefense and Emerging Infectious Diseases Consortium (National Institutes of Health Grant U54-AI-057153 (NIAID)).

REFERENCES

- Marraffini, L. A., DeDent, A. C., and Schneewind, O. (2006) *Microbiol. Mol. Biol. Rev.* **70**, 192–221
- Schneewind, O., Mihaylova-Petkov, D., and Model, P. (1993) *EMBO J.* **12**, 4803–4811
- Navarre, W. W., and Schneewind, O. (1994) *Mol. Microbiol.* **14**, 115–121
- Ton-That, H., Liu, G., Mazmanian, S. K., Faull, K. F., and Schneewind, O. (1999) *Proc. Natl. Acad. Sci. U. S. A.* **96**, 12424–12429
- Schneewind, O., Fowler, A., and Faull, K. F. (1995) *Science* **268**, 103–106
- Dramsi, S., Trieu-Cuot, P., and Bierne, H. (2005) *Res. Microbiol.* **156**, 289–297
- Connolly, K. M., Smith, B. T., Pilpa, R., Ilangovan, U., Jung, M. E., and Clubb, R. T. (2003) *J. Biol. Chem.* **278**, 34061–34065
- Mazmanian, S. K., Liu, G., Jensen, E. R., Lenoy, E., and Schneewind, O. (2000) *Proc. Natl. Acad. Sci. U. S. A.* **97**, 5510–5515
- Perry, A. M., Ton-That, H., Mazmanian, S. K., and Schneewind, O. (2002) *J. Biol. Chem.* **277**, 16241–16248
- Mazmanian, S. K., Ton-That, H., Su, K., and Schneewind, O. (2002) *Proc. Natl. Acad. Sci. U. S. A.* **99**, 2293–2298
- Marraffini, L. A., and Schneewind, O. (2005) *J. Biol. Chem.* **280**, 16263–16271
- Marraffini, L. A., and Schneewind, O. (2006) *Mol. Microbiol.* **62**, 1402–1417
- Marraffini, L. A., and Schneewind, O. (2007) *J. Bacteriol.* **189**, 6425–6436
- Ton-That, H., and Schneewind, O. (2003) *Mol. Microbiol.* **50**, 1429–1438
- Budzik, J. M., Marraffini, L. A., and Schneewind, O. (2007) *Mol. Microbiol.*

- 66, 495–510
16. Budzik, J. M., Marraffini, L. A., Souda, P., Whitelegge, J. P., Faull, K. F., and Schneewind, O. (2008) *Proc. Natl. Acad. Sci. U. S. A.* **105**, 10215–10220
 17. Kang, H. J., Coulibaly, F., Clow, F., Proft, T., and Baker, E. N. (2007) *Science* **318**, 1625–1628
 18. Oh, S. Y., Budzik, J. M., and Schneewind, O. (2008) *Proc. Natl. Acad. Sci. U. S. A.* **105**, 13703–13704
 19. Budzik, J. M., Oh, S. Y., and Schneewind, O. (2008) *J. Biol. Chem.* **283**, 36676–36686
 20. Ton-That, H., and Schneewind, O. (2004) *Trends Microbiol.* **12**, 251–261
 21. Gaspar, A. H., Marraffini, L. A., Glass, E. M., DeBord, K. L., Ton-That, H., and Schneewind, O. (2005) *J. Bacteriol.* **187**, 4646–4655
 22. Maresso, A. W., Garufi, G., and Schneewind, O. (2008) *PLoS Pathog.* **4**, e1000132
 23. Telford, J. L., Barocchi, M. A., Margarit, I., Rappuoli, R., and Grandi, G. (2006) *Nat. Rev. Microbiol.* **4**, 509–519
 24. Budzik, J. M., and Schneewind, O. (2006) *J. Clin. Investig.* **116**, 2582–2584
 25. Barocchi, M. A., Ries, J., Zogaj, X., Hemsley, C., Albiger, B., Kanth, A., Dahlberg, S., Fernebro, J., Moschioni, M., Massignani, V., Hulthenby, K., Taddei, A. R., Beiter, K., Wartha, F., von Euler, A., Covacci, A., Holden, D. W., Normark, S., Rappuoli, R., and Henriques-Normark, B. (2006) *Proc. Natl. Acad. Sci. U. S. A.* **103**, 2857–2862
 26. Manetti, A. G., Zingaretti, C., Falugi, F., Capo, S., Bombaci, M., Bagnoli, F., Gambellini, G., Bensi, G., Mora, M., Edwards, A. M., Musser, J. M., Graviss, E. A., Telford, J. L., Grandi, G., and Margarit, I. (2007) *Mol. Microbiol.* **64**, 968–983
 27. Abbot, E. L., Smith, W. D., Siou, G. P., Chiriboga, C., Smith, R. J., Wilson, J. A., Hirst, B. H., and Kehoe, M. A. (2007) *Cell. Microbiol.* **9**, 1822–1833
 28. Maisey, H. C., Hensler, M., Nizet, V., and Doran, K. S. (2007) *J. Bacteriol.* **189**, 1464–1467
 29. Dramsi, S., Caliot, E., Bonne, I., Guadagnini, S., Prevost, M. C., Kojadinovic, M., Lalioui, L., Poyart, C., and Trieu-Cuot, P. (2006) *Mol. Microbiol.* **60**, 1401–1413
 30. Mandlik, A., Swierczynski, A., Das, A., and Ton-That, H. (2007) *Mol. Microbiol.* **64**, 111–124
 31. Nelson, A. L., Ries, J., Bagnoli, F., Dahlberg, S., Falker, S., Rounioja, S., Tschop, J., Morfeldt, E., Ferlenghi, I., Hilleringmann, M., Holden, D. W., Rappuoli, R., Normark, S., Barocchi, M. A., and Henriques-Normark, B. (2007) *Mol. Microbiol.* **66**, 329–340
 32. Hilleringmann, M., Giusti, F., Baudner, B. C., Massignani, V., Covacci, A., Rappuoli, R., Barocchi, M. A., and Ferlenghi, I. (2008) *PLoS Pathog.* **4**, e1000026
 33. Edwards, A. M., Manetti, A. G., Falugi, F., Zingaretti, C., Capo, S., Buccato, S., Bensi, G., Telford, J. L., Margarit, I., and Grandi, G. (2008) *Mol. Microbiol.* **68**, 1378–1394
 34. Bagnoli, F., Moschioni, M., Donati, C., Dimitrovska, V., Ferlenghi, I., Facciotti, C., Muzzi, A., Giusti, F., Emolo, C., Sinisi, A., Hilleringmann, M., Pansegrau, W., Censini, S., Rappuoli, R., Covacci, A., Massignani, V., and Barocchi, M. A. (2008) *J. Bacteriol.* **190**, 5480–5492
 35. Huang, X., Aulabaugh, A., Ding, W., Kapoor, B., Alksne, L., Tabei, K., and Ellestad, G. (2003) *Biochemistry* **42**, 11307–11315
 36. Mishra, A., Das, A., Cisar, J. O., and Ton-That, H. (2007) *J. Bacteriol.* **189**, 3156–3165
 37. Falugi, F., Zingaretti, C., Pinto, V., Mariani, M., Amodeo, L., Manetti, A. G., Capo, S., Musser, J. M., Orefici, G., Margarit, I., Telford, J. L., Grandi, G., and Mora, M. (2008) *J. Infect. Dis.* **198**, 1834–1841
 38. Mandlik, A., Swierczynski, A., Das, A., and Ton-That, H. (2008) *Trends Microbiol.* **16**, 33–40
 39. Mandlik, A., Das, A., and Ton-That, H. (2008) *Proc. Natl. Acad. Sci. U. S. A.* **105**, 14147–14152